

Dissociation Kinetics of the GroEL–gp31 Chaperonin Complex Studied with Förster Resonance Energy Transfer[†]

Stéphane Calmat,^{‡,§} Johnny Hendriks,^{||} Harm van Heerikhuizen,[§] Christoph F. Schmidt,[⊥] Saskia M. van der Vies,[§] and Erwin J. G. Peterman^{*,‡}

[‡]Department of Physics and Astronomy and Laser Centre, VU University, Amsterdam, The Netherlands, [§]Department of Pathology, VU University Medical Center, Amsterdam, The Netherlands, ^{||}Swammerdam Institute for Life Sciences, University of Amsterdam, Amsterdam, The Netherlands, and [⊥]Drittes Physikalisches Institut, Fakultät für Physik, Georg-August-Universität, Göttingen, Germany

Received August 11, 2009; Revised Manuscript Received November 5, 2009

ABSTRACT: Propagation of bacteriophage T4 in its host *Escherichia coli* involves the folding of the major capsid protein gp23, which is facilitated by a hybrid chaperone complex consisting of the bacterial chaperonin GroEL and the phage-encoded co-chaperonin, gp31. It has been well established that the GroEL–gp31 complex is capable of folding gp23 whereas the homologous GroEL–GroES complex cannot perform this function. To assess whether this is a consequence of differences in the interactions of the proteins within the chaperonin complex, we have investigated the dissociation kinetics of GroEL–gp31 and GroEL–GroES complexes using Förster resonance energy transfer. Here we report that the dissociation of gp31 from GroEL is slightly faster than that of GroES from GroEL and is further accelerated by the binding of gp23. In contrast to what had been observed previously, we found that gp23 is able to interact with the GroEL–GroES complex, which might explain how bacteriophage T4 redirects the folding machinery of *Escherichia coli* during morphogenesis.

The GroEL–GroES chaperonin complex is absolutely required for the folding of ~3.5% of the *Escherichia coli* proteins (1) and, as a consequence, is essential for bacterial growth under all conditions tested (2). GroEL is composed of 57 kDa subunits, arranged in two heptameric rings stacked back to back. GroES is a dome-shaped heptameric ring of 10 kDa subunits that binds to the GroEL ring in the presence of nucleotides, thereby forming a cavity in which the folding of a non-native polypeptide chain is facilitated (3, 4). The folding process starts with the binding of the non-native polypeptide to one of the GroEL rings, which is then followed by binding of ATP and GroES to the same ring (*cis*), upon which the substrate is released into the GroEL–GroES cavity and starts to fold while remaining encapsulated. After hydrolysis of the ATP in the *cis* ring, ATP binds to the opposite unliganded ring (*trans*), triggering the release of GroES, ADP, and the partially or completely folded protein from the *cis* ring (5). The release of GroES is accelerated by binding of a substrate protein to the *trans* ring. The folding cycle is thought to occur with a rate of 0.12 s^{−1}, which is equal to the rate of ATP hydrolysis in the presence of GroES and excess substrate protein (6, 7).

Bacteriophages like λ and T4 utilize their host's chaperonins for the folding of their own proteins (8). Interestingly, folding of the major capsid protein of bacteriophage T4 (gp23) requires

GroEL but not GroES (9). Instead, a T4-encoded homologue of GroES, gp31, is necessary. Even though the amino acid sequences of the two proteins are only 14% identical, their overall three-dimensional structure is similar (10–13). Cryo-EM image reconstruction of the GroEL–gp31–ADP and GroEL–GroES–ADP complexes revealed that the folding cavity in the latter complex is smaller (14, 15), providing a hint about why the relatively large substrate gp23 (56 kDa) can be encapsulated only by gp31, and not by GroES (16).

In addition to a larger folding cavity, other properties of the GroEL–gp31 chaperonin complex may be required for the proper folding of gp23, including the dynamics of the interaction(s) between the different proteins in the complex. Here, we describe the kinetics of dissociation of the co-chaperonins gp31 and GroES from GroEL, and the effect of substrate proteins on dissociation using Förster resonance energy transfer (FRET).¹ We report a novel interaction between gp23 and the asymmetric GroEL–GroES chaperonin complex, as well as subtle differences between gp31 and GroES regarding their interaction with GroEL. The results are discussed in view of the requirements of the bacteriophage T4 during propagation in the *E. coli* cell.

MATERIALS AND METHODS

Production and Purification of Proteins. Plasmids encoding GroEL-315C and GroES-98C (7) under the control of an IPTG (isopropyl β -D-1-thiogalactopyranoside)-inducible promoter (kind gifts of H. Rye and A. Horwich) were used to transform *E. coli* strains MGM100 and BL21 (DE3), respectively. GroEL,

[†]This work is part of the Biomolecular Physics research program of the Stichting voor Fundamenteel Onderzoek der Materie (FOM), which is financially supported by the Nederlandse Organisatie voor Wetenschappelijk Onderzoek (NWO). C.F.S. acknowledges support by the Research Center for Molecular Physiology of the Brain, financed by the Deutsche Forschungsgemeinschaft.

*To whom correspondence should be addressed. Fax: +31 20 5987991. Telephone: +31 20 59 87576. E-mail: erwinp@nat.vu.nl.

¹Abbreviations: FRET, Förster resonance energy transfer; eGFP, enhanced green fluorescent protein; IPTG, isopropyl β -D-1-thiogalactopyranoside; TCEP, tris(2-carboxyethyl)phosphine.

GroES, GroEL-315C, GroEL D87K, GroES-98C, and gp31 were expressed and purified as previously described (16, 17). Gp23 was expressed in *E. coli* strain BL21(DE3) using IPTG-inducible plasmid pET2331 and purified as described previously (18). Purified proteins were stored in 50 mM Tris-HCl (pH 7.7), 50 mM NaCl, 1 mM EDTA, and 1 mM DTT containing 10% glycerol at -80°C .

gp31-112C was engineered by adding a cysteine residue to the C-terminus of wild-type gp31 using the QuickChange site-directed mutagenesis kit (Stratagene). The protein was expressed in *E. coli* strain MC1009 in the presence of 0.001% (w/v) L-arabinose for ~ 18 h. Cells were lysed by sonication in 100 mM KPO_4 (pH 7.4), and the cell-free extract was adjusted to a protein concentration of 8.5 mg/mL. Ammonium sulfate was added to 35% (w/v) saturation in the presence of 20% (v/v) ethanol at 25°C . After centrifugation, gp31-112C was predominantly in the supernatant. The protein solution was dialyzed against 50 mM Tris-HCl (pH 7.7) at 4°C and loaded onto a MonoQ HR 10/10 column (Pharmacia) equilibrated in 20 mM Tris-HCl (pH 8.0) and 5 mM MgCl_2 . Proteins were eluted using a NaCl gradient (0 to 1 M) in the same buffer. Fractions containing gp31-112C were pooled, concentrated (Centriprep YM-10 from Millipore), and stored at -80°C in the presence of 10% glycerol. Both GroEL-315C and gp31-112C were tested for *in vivo* folding activity as previously described (19) and were able to support the growth of bacteriophage T4 to the same extent as the wild-type proteins.

Enhanced green fluorescent protein (eGFP) was expressed in *E. coli* strain JM101 using a pTrcHisB-based plasmid (Invitrogen). After induction with 0.2 mM IPTG for ~ 18 h, cells were harvested by centrifugation, and a cell-free extract was prepared in 50 mM Tris-HCl (pH 8.0) containing 8 M urea. NiNTA agarose beads (Qiagen) were added, and the slurry was incubated at room temperature for 1 h. His-tagged eGFP (eGFP_{his}) was eluted from the beads with 50 mM Tris-HCl (pH 5.9) containing 8 M urea and 100 mM imidazole. Purified eGFP_{his} was dialyzed against 10 mM sodium phosphate buffer (pH 7.0) at 4°C and stored at -80°C .

Protein concentrations were determined by Coomassie blue-based colorimetric assay and are expressed as monomers unless otherwise stated.

Fluorescent Labeling. Proteins were reduced with 2 mM tris(2-carboxyethyl)phosphine hydrochloride (TCEP, Pierce) for 30 min at room temperature prior to labeling. A 15-fold molar excess of Atto647N-maleimide (Sigma) and a 5-fold molar excess of Cy3-maleimide (GE Healthcare) were added to GroEL-315C tetradecamers and gp31-112C (or GroES-98C) heptamers, respectively. After incubation for 1.5 h at 23°C in the dark, unreacted dye was removed by gel filtration (Sephadex G50 spin columns, Pharmacia). The number of dyes per protein was calculated using the following extinction coefficients: Atto647N-maleimide, $150000\text{ M}^{-1}\text{ cm}^{-1}$ at 644 nm; Cy3-maleimide, $150000\text{ M}^{-1}\text{ cm}^{-1}$ at 549 nm; GroEL and GroEL-315C (monomers), $9300\text{ M}^{-1}\text{ cm}^{-1}$ at 280 nm; GroES and GroES-98C (monomers), $1200\text{ M}^{-1}\text{ cm}^{-1}$ at 280 nm; gp31 and gp31-112C (monomers), $4080\text{ M}^{-1}\text{ cm}^{-1}$ at 280 nm. The extent of labeling was typically 4.3 Atto647N/GroEL tetradecamer and 1.9 Cy3/GroES (or gp31) heptamer.

Chaperonin-Assisted Refolding. All experiments were performed at 25°C . Purified eGFP_{his} was denatured in 8 mM Tris (pH 7.5), 12.5 mM HCl, 0.3 mM EDTA, and 2 mM DTT (final pH of 1.3) for 10 min. Acid-denatured eGFP_{his} was rapidly

diluted to a final concentration of $0.5\text{ }\mu\text{M}$ in a solution containing 50 mM HEPES-KOH (pH 8.0), 5 mM KCH_3COOH , 10 mM $\text{Mg}(\text{CH}_3\text{COO})_2$, 2 mM DTT, and $14\text{ }\mu\text{M}$ GroEL. The binding of eGFP_{his} to GroEL was monitored with mass spectrometry, and under these conditions, a maximum occupancy of 1 eGFP_{his}/GroEL tetradecamer was obtained. The mixture was incubated for 10 min to allow spontaneous refolding of the eGFP_{his} molecules that were not bound to GroEL. Chaperonin-assisted refolding was triggered by rapid mixing of the GroEL–eGFP_{his} complex with a solution containing $28\text{ }\mu\text{M}$ co-chaperonin and 2 mM ATP in a 1:1 ratio. After 10 min, the extent of eGFP_{his} refolding was calculated from the intensity of fluorescence at 508 nm upon excitation at 490 nm. Spontaneous eGFP_{his} refolding was monitored after rapid mixing of denatured eGFP_{his} in buffer without GroEL.

Protein Complex Formation and Dissociation Kinetics with Stopped-Flow Fluorescence. All fluorescence experiments were performed at 25°C in a solution containing 50 mM HEPES-KOH (pH 7.4), 5 mM KCH_3COOH , 10 mM $\text{Mg}(\text{CH}_3\text{COO})_2$, and 2 mM DTT using a Fluoromax-3 fluorimeter (JY-Horiba) and an RX2000 rapid-mixing accessory (Applied Photophysics), unless stated differently. Double-mixing experiments were performed with an SFA-20mxM/SPEX rapid kinetics accessory (TgK Scientific). To assess formation of the complex under steady-state conditions, Atto647N-labeled GroEL-315C (GroEL_A) and Cy3-labeled gp31-112C (gp31_D) were mixed to a final concentration of $14\text{ }\mu\text{M}$ each, in the presence or absence of 1 mM ATP. Fluorescence spectra were measured with an integration time of 50 ms per data point after excitation at 532 nm.

For determining the dissociation kinetics under steady-state conditions, GroEL_A and gp31_D were mixed to a final concentration of 180 nM , in the presence of 5 mM ATP, and loaded into the stopped-flow syringe. After rapid mixing with a 20-fold molar excess of unlabeled gp31, the fluorescence was recorded ($\lambda_{\text{exc}} = 532\text{ nm}$, $\lambda_{\text{emi}} = 665\text{ nm}$, integration time = 50 ms per data point). Typically, 10–25 traces were fitted and averaged using Origin data analysis (OriginLab Corp.). The errors quoted for the fit results are the standard deviation.

Dissociation Kinetics in the Presence of Substrate. To analyze the effect of substrates on the dissociation of co-chaperonin during steady-state ATP hydrolysis, $25\text{ }\mu\text{M}$ gp23 or MDH was denatured in 6 M urea for 2 h at 25°C . Denatured substrate was further diluted in 6 M urea to 10 or $5\text{ }\mu\text{M}$, such that the final concentration in the stopped-flow cuvette was $1\text{ }\mu\text{M}$ or 500 nM, respectively. Denatured substrate was added to GroEL_A–gp31_D–ATP complexes (prepared as stated above) in a ratio of 1:10 (v/v), immediately following the rapid addition of excess unlabeled gp31 using a double-mixing stopped-flow apparatus. To monitor the effect of substrate on the dissociation of the GroEL–gp31–ADP complex (ADP bullets), fluorescent complexes were formed by mixing $14\text{ }\mu\text{M}$ GroEL_A with $14\text{ }\mu\text{M}$ gp31_D and 1 mM ADP at 23°C for 2 h in the dark. The ADP bullets were rapidly mixed with a 10-fold molar excess of unlabeled gp31 and 4 mM ATP. The final concentrations in the cuvette were $1\text{ }\mu\text{M}$ GroEL_A, $1\text{ }\mu\text{M}$ gp31_D, $140\text{ }\mu\text{M}$ ADP, $10\text{ }\mu\text{M}$ gp31, and 2 mM ATP. Ternary complexes were formed via addition of denatured substrate to preformed GroEL–gp31–ADP complexes in five subsequent loadings to give a final total substrate:ADP bullet ratio of 1:1. The ternary complexes were incubated for 10 min at 25°C before rapid mixing with 10-fold molar excess of unlabeled gp31 and 5 mM ATP.

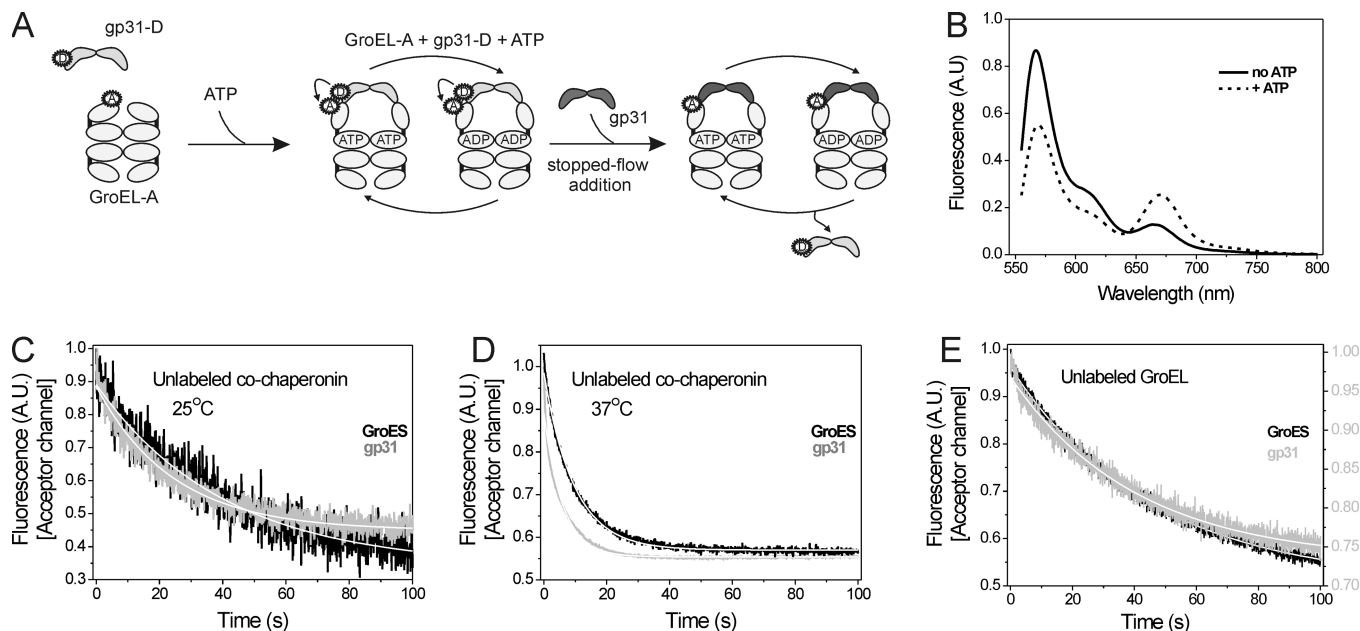


FIGURE 1: Dissociation of gp31 from GroEL during steady-state ATP hydrolysis. (A) Schematic representation of the experimental procedure. (B) Fluorescence emission spectra of a mixture of Cy3-labeled gp31 and Atto647N-labeled GroEL in the presence (---) and absence (—) of ATP. (C and D) Dissociation of fluorescent gp31 from GroEL was monitored as the decrease in the intensity of the acceptor signal at 25 and 37 °C, respectively. The data were fitted with a single-exponential decay (white superimposed lines; decay constants, $k_{3125^{\circ}\text{C}} = 0.037 \pm 0.001 \text{ s}^{-1}$, $k_{3137^{\circ}\text{C}} = 0.169 \pm 0.007 \text{ s}^{-1}$, $k_{\text{ES}25^{\circ}\text{C}} = 0.029 \pm 0.001 \text{ s}^{-1}$, and $k_{\text{ES}37^{\circ}\text{C}} = 0.105 \pm 0.004 \text{ s}^{-1}$). (E) Kinetics of dissociation of fluorescent co-chaperonins from fluorescent GroEL in the presence of excess unlabeled GroEL. The data were fitted with a single-exponential decay (white superimposed lines; decay constants, $k_{31\text{-unl}} \sim 0.025 \pm 0.001 \text{ s}^{-1}$, and $k_{\text{ES-unl}} \sim 0.022 \pm 0.001 \text{ s}^{-1}$). See also Table 1.

RESULTS

Refolding Activity of Fluorescent Chaperonin Complexes. To monitor the dissociation kinetics of GroEL and the GroES and gp31 co-chaperonins with FRET, variants of gp31, GroES, and GroEL with specific cysteine residues were generated for fluorescent labeling. A donor fluorophore (Cy3-maleimide) was attached to the C-terminus of the co-chaperonin (gp31 or GroES) on the outer rim of the dome-shaped ring (gp31_D or GroES_D). An acceptor fluorophore (Atto647N-maleimide) was attached to the apical domain of GroEL at residue 315 (GroEL_A). The positions of the fluorophores were chosen such that energy transfer only occurs when the co-chaperonin is bound to GroEL (Figure S1 of the Supporting Information). To determine whether labeling has an effect on the activity of the chaperonin complexes, the fluorescent chaperonins were analyzed for their ability to refold denatured eGFP_{his}. Because the chromophore of eGFP only fluoresces when the protein is correctly folded, eGFP is a suitable protein for monitoring chaperonin-assisted folding (20, 21). Acid-denatured eGFP_{his} was rapidly diluted in a neutral-pH buffer containing various combinations of chaperonin complexes (Figure S2A of the Supporting Information). After the refolding reaction was allowed to proceed for 10 min, the fluorescence intensity of the eGFP chromophore was determined. When acid-denatured eGFP_{his} was diluted into a buffer containing only GroEL (or GroEL_A), no refolding was observed (Figure S2B of the Supporting Information), indicating that eGFP_{his} remained bound to GroEL and did not refold spontaneously. When either co-chaperonin was added in the presence of ATP, the refolding yield of the wild-type and the fluorescent GroEL–GroES and GroEL–gp31 complexes was ~65% (Figure S2B of the Supporting Information). The kinetics of refolding were virtually identical for both the GroEL–GroES and the GroEL–gp31 complexes and different from the refolding of eGFP_{his} in the

absence of chaperonins (Figure S2C of the Supporting Information). The ability of the GroEL and gp31 mutants used here to fold their native substrate was independently confirmed with mass spectrometry (results not shown). These results show that the fluorescently labeled chaperonin proteins have refolding activity comparable to that of the wild-type proteins.

Steady-State Dynamics of the GroEL–gp31 Interaction Monitored with FRET. To gain insight into the kinetics of the GroEL–co-chaperonin interactions, we focused our attention on the dissociation of gp31 from GroEL during steady-state ATP hydrolysis (Figure 1A). First, we showed that in the presence of ATP, the donor and acceptor are close enough in the GroEL–gp31 complex to allow FRET. It has been shown that formation of a complex between GroEL and GroES occurs with a bimolecular rate constant of $\sim 5 \times 10^7 \text{ M}^{-1} \text{ s}^{-1}$ in the presence of ATP (6, 7), indicating that under our conditions (180 nM GroEL and co-chaperonin) complex formation is largely complete within a second. As one can see in Figure 1B, the donor signal (at 570 nm) is quenched whereas the acceptor signal (at 665 nm) is enhanced. Complex formation was also observed in the presence of ADP, or with the GroES co-chaperonin (data not shown). Next, the rate of dissociation of gp31 from GroEL during steady-state ATP hydrolysis was determined. A solution containing GroEL_A, gp31_D, and ATP was rapidly mixed with an excess of unlabeled gp31 at 25 °C. As expected, a decrease in the magnitude of the FRET signal was observed due to the dissociation of gp31_D from GroEL and binding of unlabeled gp31 (Figure 1C). The data were fitted with a single-exponential decay, yielding a rate constant k_{gp31} of $0.037 \pm 0.001 \text{ s}^{-1}$. Under the same conditions, the dissociation of GroES occurred with a rate constant k_{GroES} of $0.029 \pm 0.001 \text{ s}^{-1}$, which is consistent with previously reported values (7). To ensure that the subtle difference in the rate of release of GroES and gp31 was really due to the inherent properties of the two co-chaperonins and not to the

Table 1: Overview of the Rates of Dissociation of the GroES and gp31 Co-Chaperonins from GroEL

| | dissociation rate (at 25 °C) | | | | | |
|--------------------------------------|---------------------------------------|------------------------|---|------------------------|---------------------------------------|------------------------|
| | k_{fast} (s^{-1}) | relative amplitude (%) | $k_{\text{intermediate}}$ (s^{-1}) | relative amplitude (%) | k_{slow} (s^{-1}) | relative amplitude (%) |
| Steady-State ATP Hydrolysis | | | | | | |
| GroEL*–gp31* | | | | | | |
| no substrate | — | — | — | — | 0.037 ± 0.001 | — |
| 500 nM gp23 | 1.610 ± 0.008 | 35.2 | 0.211 ± 0.001 | 50.7 | 0.037 ± 0.001 | 14.1 |
| 1 μM gp23 | 2.110 ± 0.058 | 35.4 | 0.220 ± 0.017 | 57.4 | 0.037 ± 0.001 | 7.2 |
| 500 nM MDH | 1.390 ± 0.164 | 37.5 | 0.239 ± 0.016 | 46.6 | 0.037 ± 0.001 | 15.9 |
| 1 μM MDH | 2.170 ± 0.149 | 33.3 | 0.228 ± 0.002 | 56.9 | 0.037 ± 0.001 | 9.8 |
| GroEL*–GroES* | | | | | | |
| no substrate | — | — | — | — | 0.029 ± 0.001 | — |
| 200 nM gp23 | 0.871 ± 0.167 | 37.5 | 0.212 ± 0.016 | 25.2 | 0.029 ± 0.001 | 37.3 |
| Preformed GroEL*–gp31*–ADP Complexes | | | | | | |
| no substrate | — | — | — | — | 0.035 ± 0.001 | — |
| 500 nM gp23 | 0.274 ± 0.024 | 54.4 | — | — | 0.035 ± 0.001 | 45.6 |
| 1 μM gp23 | 0.257 ± 0.022 | 52 | — | — | 0.035 ± 0.001 | 48 |

presence of contaminating peptides in the co-chaperonin stock solutions, the experiment was repeated in the presence of GroEL “trap”, a mutant GroEL protein (GroELD87K), which binds but cannot release bound proteins or peptides (22). Under conditions where any residual unfolded protein that could be present in the stocks of co-chaperonins binds to the GroEL trap, the rate of release of gp31 from GroEL was 1.1-fold faster than for GroES (data not shown). At the physiologically more relevant temperature of 37 °C, the dissociation of both co-chaperonins from GroEL was faster and the dissociation rate of gp31 was 60% faster than that of GroES [$k_{\text{gp31}} = 0.169 \pm 0.007 \text{ s}^{-1}$, and $k_{\text{GroES}} = 0.105 \pm 0.004 \text{ s}^{-1}$ (Figure 1D)]. Similar results were obtained when the increase in donor fluorescence was monitored over time (data not shown). The data show that during steady-state ATP turnover, gp31 is released from GroEL faster than GroES is released (Table 1). The experiments discussed so far do not allow discrimination between release of the co-chaperonin before or after binding of an additional co-chaperonin to the *trans* ring of GroEL. To test this, measurements were performed monitoring the decrease in the level of FRET via addition of unlabeled GroEL to labeled GroEL–co-chaperonin complexes (Figure 1E). The rate constants of the decrease in the magnitude of the acceptor signal obtained in this way were similar to those obtained before using unlabeled co-chaperonin, which strongly suggests that, under these experimental conditions, co-chaperonin release occurs before binding of a new co-chaperonin.

Effect of gp23 Binding on the Rates of Dissociation of gp31 and GroES from GroEL. In previous studies, dissociation of GroES from cycling GroEL–GroES complexes (i.e., during steady-state ATP hydrolysis) in the presence of substrate was shown to proceed with two rates (7, 23): a slow rate, corresponding to co-chaperonin release during steady-state ATP turnover, and a fast rate, reflecting dissociation of GroES from ADP bullets that have undergone a conformational change in the *cis* ring following ATP hydrolysis (“activated” ADP bullets). This conformational change is thought to be the rate-limiting step controlling the release of the co-chaperonin in the absence of a substrate protein (7). Binding of a substrate protein to the GroEL *trans* ring induces the formation of activated

bullets, resulting in fast co-chaperonin release kinetics in a concentration-dependent manner (7). To determine whether the binding of gp23 to the *trans* ring of cycling GroEL–gp31 complexes affects the dissociation kinetics of gp31, a solution containing GroEL_A, gp31_D, and ATP was rapidly mixed with an excess of unlabeled gp31, immediately followed by the addition of urea-denatured gp23 using a double-mixing stopped-flow apparatus (Figure 2A).

In contrast to what was observed in the absence of gp23, the dissociation of gp31 from GroEL occurred with three distinct rates: $k_{\text{slow}} = 0.037 \pm 0.001 \text{ s}^{-1}$, $k_{\text{fast}} = 2.110 \pm 0.058 \text{ s}^{-1}$, and $k_{\text{intermediate}} = 0.220 \pm 0.017 \text{ s}^{-1}$ (Figure 2B and Table 1). Three exponentials were required to properly fit the data, as can be judged from the residuals (Figure S3 of the Supporting Information). To assess whether the effect of gp23 on the dissociation kinetics is comparable to the effect of other substrates, we analyzed the effect of urea-denatured MDH on the dissociation of gp31 from GroEL. As one can see in Figure 3B and Table 1, the effect of MDH on the dissociation kinetics was similar to that of gp23. Although the affinity of MDH for free GroEL was shown to be higher than that of gp23 using mass spectrometry (24), it is possible that in the presence of co-chaperonin, the difference in the affinity of the two substrates for the *trans* ring of GroEL is reduced, explaining the comparable effect of MDH and gp23 on the co-chaperonin dissociation kinetics. It should be noted that a 2-fold increase in the denatured substrate concentration had no effect on the dissociation rates but did have an influence on the amplitudes. With increasing amounts of denatured gp23 or MDH, the amplitude of the slow component decreased while that of the intermediate component increased (Table 1). The presence of denatured gp23 also had an accelerating effect on the dissociation of preformed GroEL–gp31–ADP complexes, which occurred with two exponential rates: $k_{\text{fast-ADP}} = 0.257 \pm 0.022 \text{ s}^{-1}$, and $k_{\text{slow-ADP}} = 0.035 \pm 0.001 \text{ s}^{-1}$ (Figure 2C,D and Table 1).

The slow rate constant k_{slow} ($\sim 0.04 \text{ s}^{-1}$), determined during steady-state ATP hydrolysis, is similar to the dissociation rate constant obtained in the absence of substrate (Table 1). Furthermore, the amplitude decreased with an increase in substrate

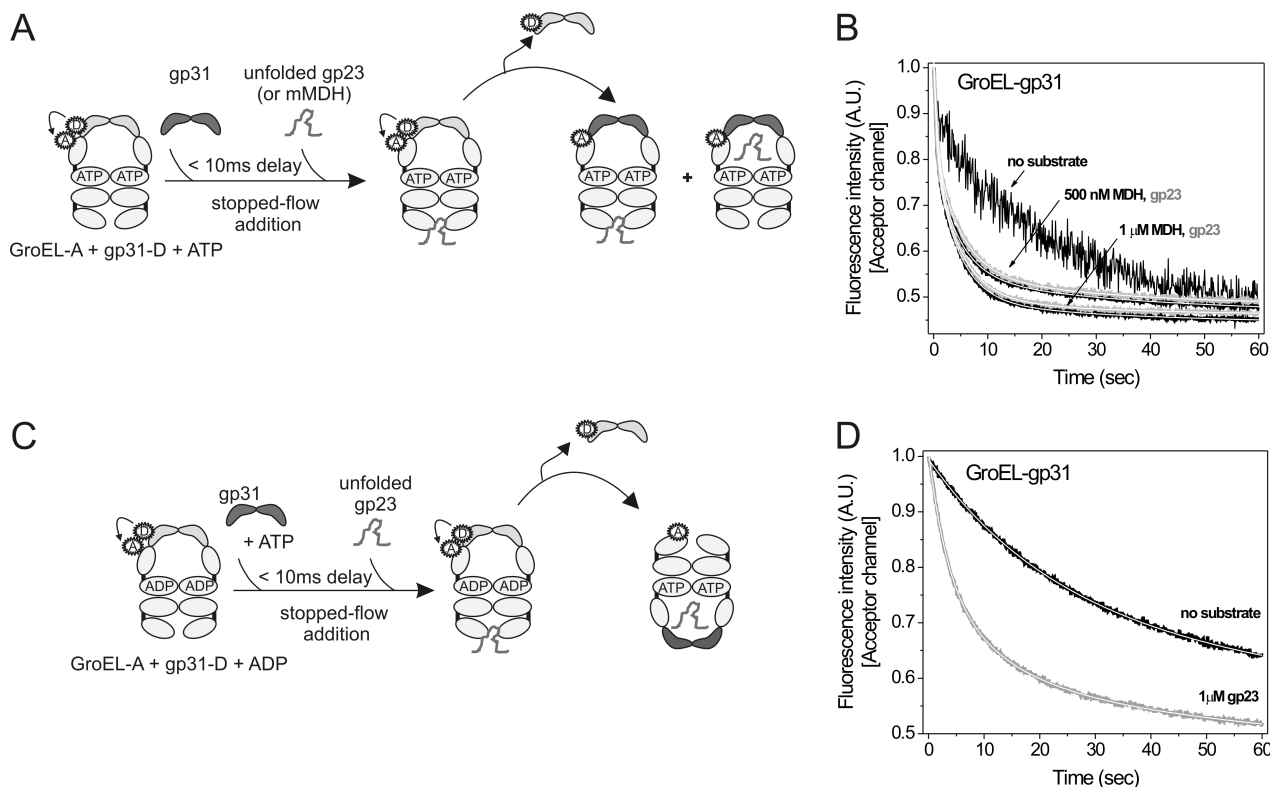


FIGURE 2: Effect of substrate on the dissociation of gp31 from GroEL. (A and C) Schematic representations of the experimental procedures. (B) Dissociation of fluorescent gp31 from GroEL during steady-state ATP hydrolysis, shown as the decrease in intensity of the acceptor signal, in the presence of increasing concentrations of denatured gp23 (gray) or malate dehydrogenase (black). The data were fitted with a triple-exponential decay (white superimposed lines; decay constants, $k_{\text{slow}} = 0.037 \pm 0.001 \text{ s}^{-1}$, $k_{\text{fast}} = 2.110 \pm 0.058 \text{ s}^{-1}$, and $k_{\text{intermediate}} = 0.220 \pm 0.017 \text{ s}^{-1}$). Note the trace in the absence of substrate is the same gp31 dissociation trace as in Figure 1C. (D) Dissociation of fluorescent gp31 from preformed ADP bullets in the absence (black) or presence (gray) of denatured gp23. The data were fitted with a double-exponential decay (white superimposed lines; decay constants, $k_{\text{slow-ADP}} = 0.035 \pm 0.001 \text{ s}^{-1}$, and $k_{\text{fast-ADP}} = 0.220 \pm 0.017 \text{ s}^{-1}$). See also Table 1 and Figure S3 of the Supporting Information.

concentration. Taken together, these observations indicate that k_{slow} corresponds to the dissociation of gp31 from GroEL to which no gp23 is bound (Figure 1). In a similar study, dissociation of the co-chaperonin from GroEL–GroES ADP bullets was observed with a rate constant of $1\text{--}2 \text{ s}^{-1}$ (7). This rate was interpreted to reflect dissociation of GroES from GroEL–GroES–ADP complexes having undergone a conformational change in the *cis* ring, as a result of ATP hydrolysis (activated bullets). It is thus likely that the comparable rate constant we observed ($k_{\text{fast}} \sim 2 \text{ s}^{-1}$) corresponds to gp31 dissociating from similarly activated GroEL–gp31–ADP bullets (Figure 4). Finally, the third event (with a rate constant $k_{\text{intermediate}}$ of $\sim 0.2 \text{ s}^{-1}$) occurs on the same time scale as ATP hydrolysis by GroEL in the presence of GroES and denatured substrate (7) and might hence reflect the rate of ATP hydrolysis of cycling GroEL–gp31 complexes in the presence of gp23 (Figure 4). The observation that increasing amounts of denatured substrate increase the prevalence of $k_{\text{intermediate}}$ suggests that *in vivo*, the presence of non-native substrate (i.e., newly synthesized gp23 during bacteriophage T4 infection) may influence the GroEL–gp31 folding cycle so that the overall rate would correspond to a $k_{\text{intermediate}}$ of $\sim 0.2 \text{ s}^{-1}$ (Figure 4).

In a previous study using size-exclusion chromatography and immunodetection, ternary complexes of gp23 bound to the *trans* ring of preformed GroEL–GroES–ADP complexes were not observed (16). However, here we show that gp23 has an accelerating effect on the dissociation kinetics of cycling GroEL–GroES–ATP complexes (Figure 3 and Table 1), hinting about an

interaction of gp23 with the *trans* ring of the GroEL–GroES complex. To confirm the binding of gp23 to the *trans* ring of GroEL–GroES complexes, we performed a FRET experiment. To this end, fluorescently labeled gp23 (gp23_D) was denatured in urea and added to a solution containing GroEL_A, unlabeled GroES, and ADP (Figure 3 C). A 10-fold excess of unlabeled GroES relative to GroEL_A was used, to ensure that all GroEL_A was in complex with GroES. Upon addition of gp23_D, a decrease in the gp23 donor fluorescence intensity and an increase in the GroEL acceptor fluorescence intensity were observed (Figure 3D), indicating the occurrence of FRET. Identical results were observed when ATP or when labeled gp31 was used. Collectively, these findings show that the bacteriophage T4 major capsid protein can bind to the *trans* ring of GroEL–GroES asymmetric complexes.

DISCUSSION

We have shown that the kinetics of dissociation of gp31 from cycling GroEL–gp31 complexes are faster than those of GroES and that the binding of the natural substrate protein gp23 to the *trans* ring of the GroEL–gp31 complex accelerates the release of gp31 (Table 1). In contrast to what has been reported previously, we find that gp23 can bind to the *trans* ring of the GroEL–GroES complex (16). It is interesting to consider that during T4 infection of *E. coli* the demand for chaperonin-assisted folding is very high. Most of the GroEL is expected to be in complex with gp31 by the time gp23 is synthesized; however, some GroEL–GroES complexes may still be present. Binding of gp23 to these

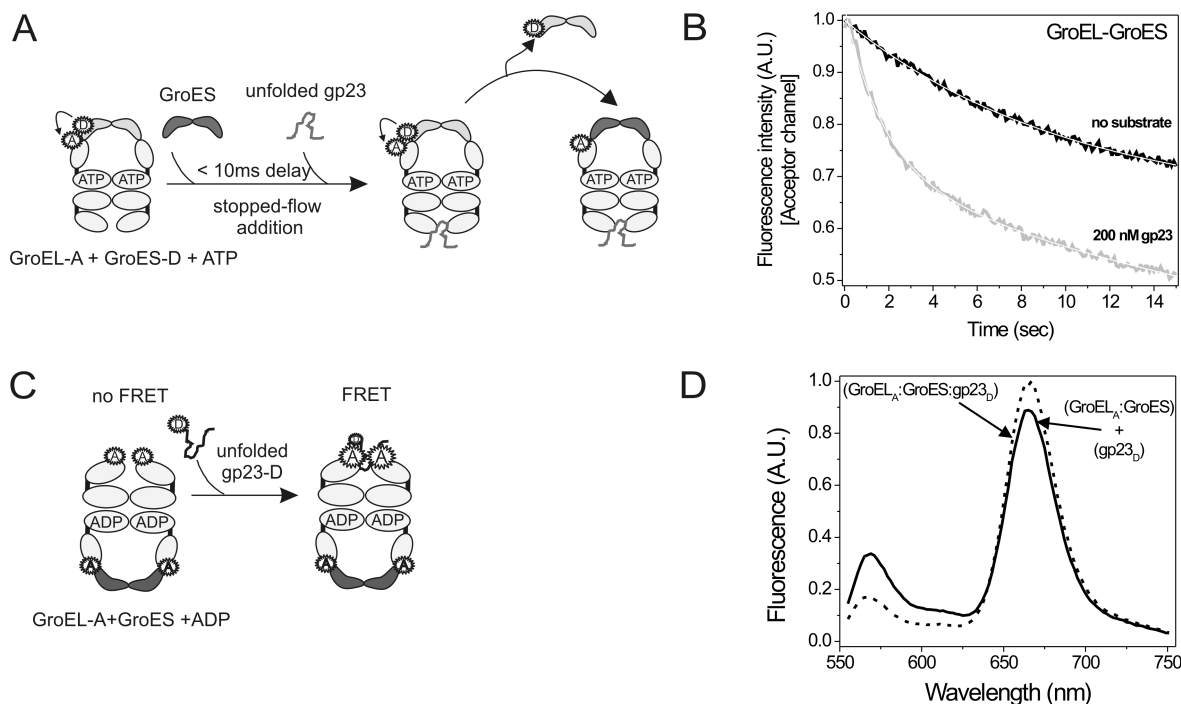


FIGURE 3: Binding of gp23 to GroEL–GroES complexes. (A) Schematic representation of the dissociation of GroES from GroEL in presence of gp23. (B) Dissociation of GroES from GroEL during steady-state ATP hydrolysis in the absence (black) and presence of denatured gp23 (gray). The data were fitted with a triple-exponential decay (white superimposed lines; decay constants, $k_{\text{slow}} = 0.029 \pm 0.001 \text{ s}^{-1}$, $k_{\text{fast}} = 0.871 \pm 0.167 \text{ s}^{-1}$, and $k_{\text{intermediate}} = 0.212 \pm 0.016 \text{ s}^{-1}$). See also Table 1. Note the trace in the absence of substrate is the same GroES dissociation trace as in Figure 1C. (C) Schematic representation of the binding experiment. (D) Sum of the emission spectrum of a solution of urea-denatured Cy3-labeled gp23 and the emission spectrum of a solution containing urea-denatured Cy3-labeled gp23 preincubated with Atto647N-labeled GroEL in complex with GroES and ATP (—). Emission spectrum of a solution containing urea-denatured Cy3-labeled gp23 preincubated with Atto647N-labeled GroEL in complex with GroES and ADP (---). Note here the sum of the emission spectra of the two solutions was used to determine the “theoretical” spectrum of unbound denatured fluorescent gp23 in the presence of fluorescent GroEL, since the addition of denatured gp23 to a solution containing GroEL would have resulted in binding, and therefore FRET.

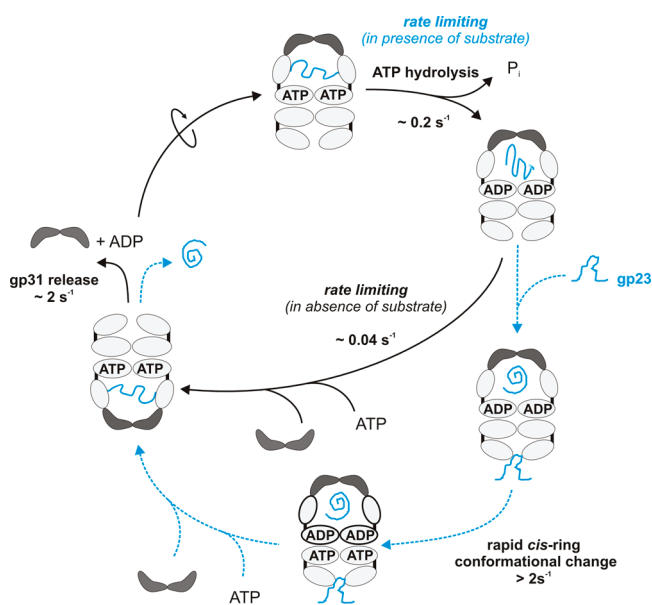


FIGURE 4: Proposed model for cycling of the GroEL–gp31 chaperonin complex in the absence and presence of gp23. In the absence of substrate (black arrows), the GroEL–gp31 chaperonin complex dissociates slowly, with an overall rate of $\sim 0.04 \text{ s}^{-1}$. In the presence of its physiological substrate gp23 (blue arrows), the GroEL–gp31 chaperonin complex dissociates very rapidly ($\sim 2 \text{ s}^{-1}$), ensuring an overall cycle rate of $\sim 0.2 \text{ s}^{-1}$ (ATP hydrolysis becomes the rate-limiting step).

latter endogenous chaperonin complexes will accelerate the dissociation of the GroES co-chaperonin (incompetent for the

folding of the major capsid protein) and allow binding of gp31, required for gp23 folding (14, 15).

In the absence of substrate proteins, we find that the dissociation rate of gp31 is faster than that of GroES ($k_{\text{gp31}} = 0.037 \pm 0.001 \text{ s}^{-1}$, and $k_{\text{GroES}} = 0.029 \pm 0.001 \text{ s}^{-1}$). Although this difference is statistically significant, it remains unclear whether it is important for chaperonin function. The difference could be caused by slightly different interactions of gp31 with GroEL compared to those of GroES, possibly as a result of the different amino acids in the co-chaperonin mobile loops that interact with GroEL (10). This is supported by the report that mutations in the mobile loop of gp31 influence the affinity and binding kinetics of gp31 and GroEL (25).

In the presence of substrate protein, we show that dissociation of gp31 is greatly accelerated ($k_{\text{intermediate}} = 0.220 \pm 0.017 \text{ s}^{-1}$). We infer that under saturating substrate concentrations, the GroEL–gp31 cycle occurs at a rate of $\sim 0.2 \text{ s}^{-1}$, which is likely the rate of ATP hydrolysis, similar to the GroEL–GroES cycle (7). How does this GroEL–gp31 cycling rate of 0.2 s^{-1} relate to the required rate of gp23 folding *in vivo*? During infection by T4, one *E. coli* cell produces on average 200 progeny phages. Each bacteriophage prohead consists of 930 gp23 copies (26, 27), so at least 186000 gp23 molecules have to be folded in $\sim 10 \text{ min}$, which is the time between the start of gp23 synthesis and cell lysis required for release of progeny phages (28). An infected *E. coli* cell contains 1600 GroEL tetradecamers, 3000 GroES heptamers, and 7800 gp31 heptamers (29, 30). Note that host protein synthesis shuts down after infection and gp23 is by far the most abundant newly synthesized protein. This implies

that GroEL is exclusively folding gp23 and that one GroEL–gp31 complex folds on average ~ 120 gp23 molecules in ~ 10 min; i.e., the chaperonin-assisted folding rate of gp23 in the cell should be $\sim 0.2\text{ s}^{-1}$. Here we show that the cycling rate of the GroEL–gp31 complex in the presence of excess physiological substrate is $\sim 0.2\text{ s}^{-1}$, which is close to the estimate of the folding rate of gp23 required in vivo. This observation suggests that a GroEL–gp31 cycling rate of $\sim 0.2\text{ s}^{-1}$ would be sufficient to fulfill the in vivo requirement for gp23 folding only if the efficiency, which is unknown, would be close to unity. Here, efficiency is defined as the fraction of GroEL-bound substrate molecules that are fully folded in one folding cycle consisting of encapsulation by co-chaperonin, ATP hydrolysis, and release of co-chaperonin and substrate. In other words, we infer that the folding of gp23 inside the GroEL–gp31 complex is largely complete before release of the co-chaperonin. It will be interesting to determine the rate of gp23 folding in the GroEL–gp31 chaperonin complex directly to further dissect the adapting nature of bacteriophage T4. The data we have presented here show that the need for the co-chaperonin gp31 to fold gp23 does not appear to reside in differences between the intrinsic kinetics and mechanism of the GroEL–gp31 complex compared to the GroEL–GroES complex. Instead, the cavity size, physicochemical nature of the cavity, and/or specific properties of gp23 itself are more likely to be the parameters of importance.

ACKNOWLEDGMENT

We thank Art Horwich and Hays Rye for the plasmids encoding GroEL315C and GroES98C, Wayne Fenton for the plasmid encoding GroELD87K, Chris Vos for the *E. coli* strain expressing eGFP_{his}, and Patrick Bakkes for helpful discussions.

SUPPORTING INFORMATION AVAILABLE

Supplemental Figure S1, Figure S2, and Figure S3. This material is available free of charge via the Internet at <http://pubs.acs.org>.

REFERENCES

- Kerner, M. J., Naylor, D. J., Ishihama, Y., Maier, T., Chang, H. C., Stines, A. P., Georgopoulos, C., Frishman, D., Hayer-Hartl, M., Mann, M., and Hartl, F. U. (2005) Proteome-wide analysis of chaperonin-dependent protein folding in *Escherichia coli*. *Cell* 122, 209–220.
- Fayet, O., Ziegelhoffer, T., and Georgopoulos, C. (1989) The groES and groEL heat shock gene products of *Escherichia coli* are essential for bacterial growth at all temperatures. *J. Bacteriol.* 171, 1379–1385.
- Chen, S., Roseman, A. M., Hunter, A. S., Wood, S. P., Burston, S. G., Ranson, N. A., Clarke, A. R., and Saibil, H. R. (1994) Location of a Folding Protein and Shape Changes in GroEL–GroES Complexes Imaged by Cryo-electron Microscopy. *Nature* 371, 261–264.
- Xu, Z. H., Horwich, A. L., and Sigler, P. B. (1997) The crystal structure of the asymmetric GroEL–GroES–(ADP)(7) chaperonin complex. *Nature* 388, 741–750.
- Horwich, A. L., Farr, G. W., and Fenton, W. A. (2006) GroEL–GroES-mediated protein folding. *Chem. Rev.* 106, 1917–1930.
- Burston, S. G., Ranson, N. A., and Clarke, A. R. (1995) The Origins and Consequences of Asymmetry in the Chaperonin Reaction Cycle. *J. Mol. Biol.* 249, 138.
- Rye, H. S., Roseman, A. M., Chen, S. X., Furtak, K., Fenton, W. A., Saibil, H. R., and Horwich, A. L. (1999) GroEL–GroES cycling: ATP and nonnative polypeptide direct alternation of folding-active rings. *Cell* 97, 325–338.
- Ang, D., Keppel, F., Klein, G., Richardson, A., and Georgopoulos, C. (2000) Genetic analysis of bacteriophage-encoded co-chaperonins. *Annu. Rev. Genet.* 34, 439–456.
- Georgopoulos, C., Kaiser, A. D., and Wood, W. B. (1972) Role of Host-Cell in Bacteriophage Morphogenesis: Effects of a Bacterial Mutation on T4 Head Assembly. *Nature* 239, 38–41.
- Hunt, J. F., van der Vies, S. M., Henry, L., and Deisenhofer, J. (1997) Structural Adaptations in the Specialized Bacteriophage T4 Co-chaperonin Gp31 Expand the Size of the Anfinsen Cage. *Cell* 90, 361–371.
- Koonin, E. V., and van der Vies, S. M. (1995) Conserved Sequence Motifs in Bacterial and Bacteriophage Chaperonins. *Trends Biochem. Sci.* 20, 14–15.
- Laemmli, U. K., Beguin, F., and Gujerker, G. (1970) A Factor Preventing Major Head Protein of Bacteriophage T4 from Random Aggregation. *J. Mol. Biol.* 47, 69–85.
- van der Vies, S. M., Gatenby, A. A., and Georgopoulos, C. (1994) Bacteriophage T4 Encodes a Co-chaperonin that can Substitute for *Escherichia coli* GroES in Protein Folding. *Nature* 368, 654–656.
- Clare, D. K., Bakkes, P. J., van Heerikhuizen, H., van der Vies, S. M., and Saibil, H. R. (2006) An Expanded Protein Folding Cage in the GroEL–gp31 Complex. *J. Mol. Biol.* 358, 905–911.
- Clare, D. K., Bakkes, P. J., van Heerikhuizen, H., van der Vies, S. M., and Saibil, H. R. (2009) Chaperonin Complex with a Newly Folded Protein Encapsulated in the Folding Chamber. *Nature* 457, 107–113.
- Bakkes, P. J., Faber, B. W., van Heerikhuizen, H., and van der Vies, S. M. (2005) The T4-Encoded Co-chaperonin, gp31, has Unique Properties that Explain its Requirement for the Folding of the T4 Major Capsid Protein. *Proc. Natl. Acad. Sci. U.S.A.* 102, 8144–8149.
- van der Vies, S. M. (2000) Purification of the Gp31 Co-chaperonin of Bacteriophage T4. *Methods Mol. Biol.* 140, 51–61.
- van Duijn, E., Bakkes, P. J., Heeren, R. M. A., van den Heuvel, R. H. H., van Heerikhuizen, H., van der Vies, S. M., and Heck, A. J. R. (2005) Monitoring Macromolecular Complexes Involved in the Chaperonin-Assisted Protein Folding Cycle by Mass Spectrometry. *Nat. Methods* 2, 371–376.
- Tilly, K., and Georgopoulos, C. (1982) Evidence that the Two *Escherichia coli* GroE Morphogenetic Gene Products Interact In Vivo. *J. Bacteriol.* 149, 1082–1088.
- Makino, Y., Amada, K., Taguchi, H., and Yoshida, M. (1997) Chaperonin-Mediated Folding of Green Fluorescent Protein. *J. Biol. Chem.* 272, 12468–12474.
- Weissman, J. S., Rye, H. S., Fenton, W. A., Beechem, J. M., and Horwich, A. L. (1996) Characterization of the Active Intermediate of a GroEL–GroES-Mediated Protein Folding Reaction. *Cell* 84, 481–490.
- Fenton, W. A., Kashi, Y., Furtak, K., and Horwich, A. L. (1994) Residues in Chaperonin GroEL Required for Polypeptide Binding and Release. *Nature* 371, 614–619.
- Fridmann, Y., Kafri, G., Danziger, O., and Horovitz, A. (2002) Dissociation of the GroEL–GroES Asymmetric Complex is Accelerated by Increased Cooperativity in ATP Binding to the GroEL Ring Distal to GroES. *Biochemistry* 41, 5938–5944.
- Van Duijn, E., Heck, A. J. R., and Van Der Vies, S. M. (2007) Inter-Ring Communication Allows the GroEL Chaperonin Complex to Distinguish Between Different Substrates. *Protein Sci.* 16, 956–965.
- Richardson, A., van der Vies, S. M., Keppel, F., Taher, A., Landry, S. J., and Georgopoulos, C. (1999) Compensatory Changes in GroEL/Gp31 Affinity as a Mechanism for Allele-Specific Genetic Interaction. *J. Biol. Chem.* 274, 52–58.
- Baschong, W., Aebi, U., Baschongprescianotto, C., Dubochet, J., Landmann, L., Kellenberger, E., and Wurtz, M. (1988) Head Structure of Bacteriophage-T2 and Bacteriophage-T4. *J. Ultrastruct. Mol. Struct. Res.* 99, 189–202.
- Fokine, A., Chipman, P. R., Leiman, P. G., Mesyanzhinov, V. V., Rao, V. B., and Rossmann, M. G. (2004) Molecular Architecture of the Prolate Head of Bacteriophage T4. *Proc. Natl. Acad. Sci. U.S.A.* 101, 6003–6008.
- Karam, J. D., and Drake, J. W. (1994) Molecular biology of bacteriophage T4, American Society for Microbiology, Washington, DC.
- Castillo, C. J., and Black, L. W. (1978) Purification and Properties of Bacteriophage-T4 Gene-31 Protein Required for Prehead Assembly. *J. Biol. Chem.* 253, 2132–2139.
- Lorimer, G. H. (1996) A Quantitative Assessment of the Role of the Chaperonin Proteins in Protein Folding In Vivo. *FASEB J.* 10, 5–9.